Electronic Supplementary Material (ESI) for ChemComm.

Supporting Information

Light-mediated chiroptical switching of an achiral foldamer host in presence of a carbohydrate guest

Susnata Pramanik,[a] Brice Kauffmann,[b] Stefan Hecht,[c] Yann Ferrand,[d] Ivan Huc,*[a]

[a]Department Pharmazie and Center for Integrated Protein Science, Ludwig-Maximilians-Universität, Butenandtstr. 5–13, 81377 München (Germany).

[b]Université de Bordeaux CNRS, INSERM, UMS3033, Institut Européen de Chimie et Biologie (IECB), 2 rue Robert Escarpit, 33600 Pessac (France).

[c]Institute of Technical and Macromolecular Chemistry, RWTH Aachen University, Worringer Weg 2, 52074 Aachen (Germany).

[d]CBMN (UMR5248), Univ. Bordeaux—CNRS—IPB, Institut Européen de Chimie et Biologie, 2 rue Robert Escarpit, 33600 Pessac (France).

*Correspondence to:

ivan.huc@cup.lmu.de

Table of Contents

1. Synthesis

1.1 General information:

Commercially available reagents were used without further purification. Tetrahydrofurane (THF), dichloromethane (CH_2Cl_2) and toluene were dried over alumina columns; chloroform, triethylamine and diisopropylethylamine (DIEA) were distilled over calcium hydride (CaH_2) prior to use. Reactions were monitored by thin layer chromatography (TLC) on Merck silica gel 60-F254 plates and observed under UV light. Column chromatography purifications were carried out on Merck GEDURAN Si60 (40-63 µm). Preparative recycling GPC (gel permeation chromatography) was carried out on JAIGEL 20*600 mm columns (Japan Analytical Industry) in chloroform containing 1% ethanol and 0.5% triethylamine as mobile phase, with a flow rate of 7.5 mL/min. Monitoring by UV detection was carried out at 254 nm, 280 nm, 300 nm and 360 nm. Nuclear magnetic resonance (NMR) spectra were recorded on Bruker Avance 400 and 500 MHz and Varian 600 MHz spectrometers using the deuterated solvent as the lock and residual solvent as the internal reference. The multiplicity of the signal is provided as singlet (s), doublet (d), triplet (t), doublet of doublets (dd), doublet of doublets of doublets (ddd), doublet of triplets (dt), triplet of doublets (td), multiplet (m), broad singlet (bs), broad unsplitted signal (b). ESI-HRMS mass spectra were measured on *Thermo Finnigan LTQ-FT* at LMU Munich facility and *Thermo Exactive orbitrap* instrument from the Mass Spectrometry Laboratory at the European Institute of Chemistry and Biology (UMS 3033 - IECB), Pessac, France. UV-vis spectra were measured on a Cary 50. Illumination was performed using a Till Photonics Polychrome 5000 monochromator equipped with a 150 Watt Xenon short arc lamp. A 365 nm filter with a bandwidth of 15 nm and another light source with a cut off wavelength of >450 nm were used. Chloroform was distilled over CaH_2 and stored under N_2 prior to use. DMSO was used as received. A mixture of $CDCl_3$ and DMSO-d_6 was taken in an NMR tube and purged with N_2 (ca. 10 min) before NMR experiments were performed.

1.2 Synthetic Scheme

Scheme S1: Synthesis of photoswitches **5** and **6**

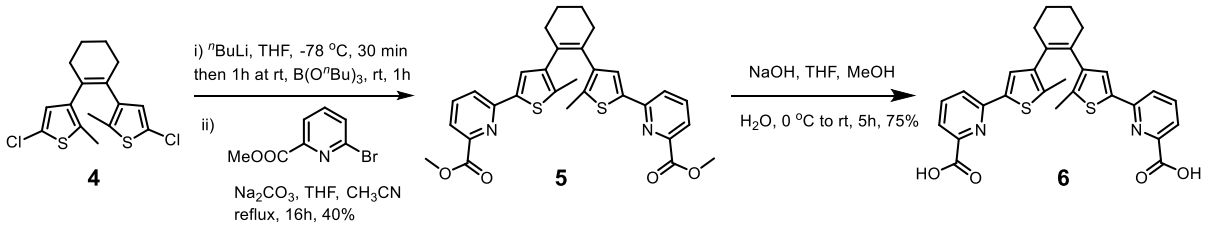

Scheme S2: Synthesis of capsules **1** and **2**

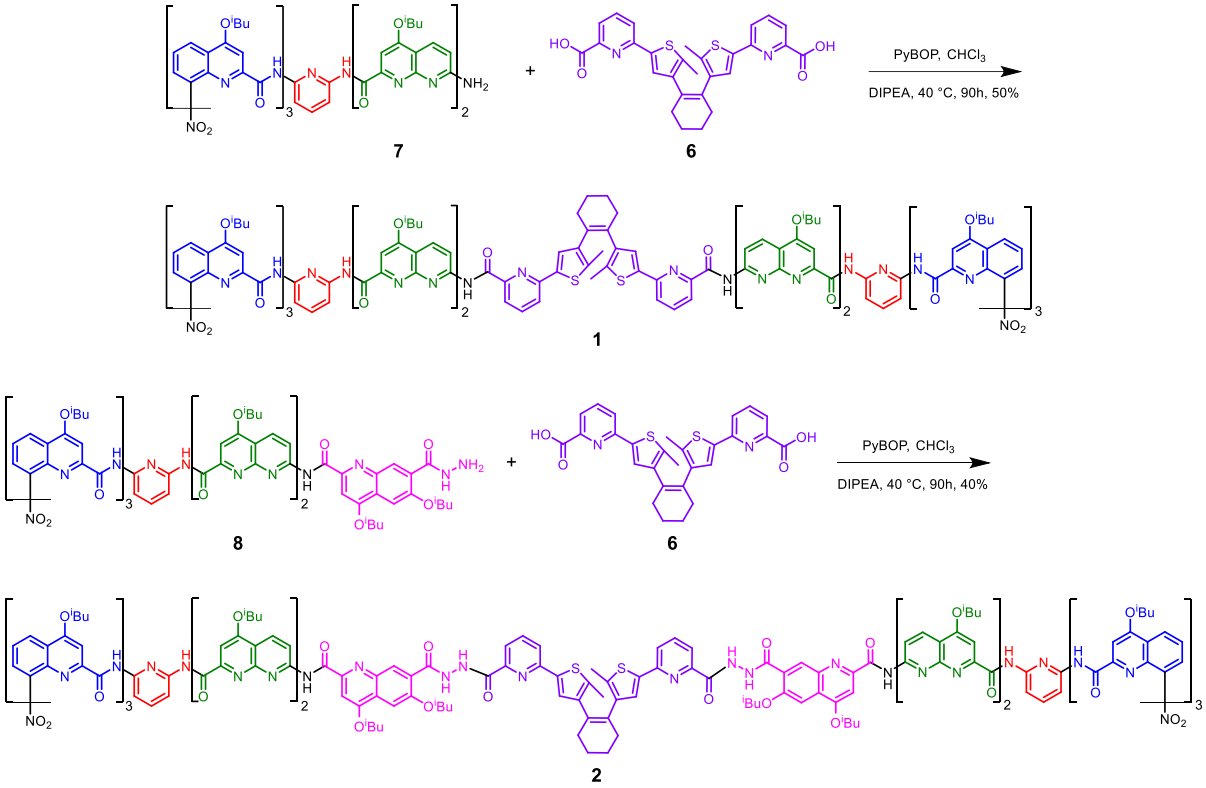

1.3 Experimental procedure:

Photoswitch 5. ^{n}BuLi (2.5 M, 0.40 mL, 1.00 mmol) was added dropwise to a solution of **4**[S1] (140 mg, 0.41 μmol) in dry THF (5 mL) at -78 °C. After stirring the mixture at the same temperature for 30 min, the solution was warmed to room temperature and stirred for additional 1 h prior to the addition of tributyl borate (0.30 mL, 1.11 mmol). The resulting mixture was stirred 1 h and then quenched with saturated aq. $NaHCO_3$, extracted with DCM (3 × 10 mL), dried over Na_2SO_4 and evaporated. To the crude mixture methyl 6-bromopicolinate (221 mg, 1.10 mmol), and Na_2CO_3 (3.73 g, 35.2 mmol) were added and taken in acetonitrile (10 mL) and THF (8 mL) mixture of solvents. Molecular oxygen was removed using freeze-pump-thaw process (three times) and $Pd(PPh_3)_4$ (51 mg, 44 μmol) was added. After refluxing for 16h, solvents were removed and the crude was redissolved in DCM. Organic phase was washed with water, dried and evaporated. The crude was purified by column chromatography using 20% ethyl acetate in cyclohexane furnishing off white solid (90 mg, 160 μmol, 40%). ^{1}H NMR (400 MHz, $CDCl_3$) δ 7.88 (dd, *J* = 7.6, 1.2 Hz, 2H); 7.72 (t, *J* = 7.6 Hz, 2H); 7.59 (dd, *J* = 7.6, 1.2 Hz, 2H), 7.33, (s, 2H), 3.98 (s, 6H), 2.42-2.39 (m, 4H); 2.07 (s, 6H), 1.85-1.82 (m, 4H). ^{13}C NMR (100 MHz, $CDCl_3$) δ 165.9, 153.1, 147.9, 141.6, 138.7, 137.7, 137.5, 131.8, 127.4, 122.6, 121.7, 77.5, 53.6, 53.0, 31.8, 23.4, 14.8 ppm. HRMS (ESI^+): m/z calcd for $C_{30}H_{29}N_2O_4S_2$ $[M+H]^+$ 545.1563 found 545.1562.

Photoswitch 6. Compound **5** (90 mg, 0.16 mmol) was dissolved in THF (5 mL) and methanol (2 mL) mixture of solvents and followed by the addition of aq. NaOH (26 mg, 0.66 mmol, in 2 mL of water). After 5 h of stirring at room temperature, solvents were removed and neutralized with 1M HCl. 20 mL of water was added and the product was extracted with DCM (3 × 10 mL), dried and evaporated furnishing light purple solid (62 mg, 0.12 mmol, 75%). ^{1}H NMR (400 MHz, $CDCl_3$) δ 7.99 (dd, *J* = 7.6, 0.8 Hz, 2H); 7.86 (t, *J* = 7.6 Hz, 2H); 7.69 (dd, *J* = 7.6, 0.8 Hz, 2H), 7.33, (s, 2H), 2.43-2.40 (m, 4H); 2.13 (s, 6H), 1.88-1.85 (m, 4H). ^{13}C NMR (126 MHz, DMSO-d_6) δ 165.9, 152.0, 148.2, 141.3, 138.5, 138.2, 136.6, 131.2, 127.9, 122.4, 121.2, 40.0, 31.1, 22.6, 14.3 ppm. HRMS (ESI^+): m/z calcd for $C_{28}H_{25}N_2O_4S_2$ $[M+H]^+$ 517.1250 found 517.1249.

General procedure for the synthesis of capsules: Oligomer amine (**7**[S2] for capsule **1** and **8**[S3] for capsule **2**, 2 equiv.), diacid **6** (1 equiv.) and PyBOP (6 equiv.) were dissolved in dry $CHCl_3$ (2 mL) and followed by the addition of DIPEA (6 equiv.). After 90 h of stirring at 40 °C, solvent was removed and the residue was purified by GPC. The fraction collected was washed with 1% aqueous citric acid and followed by brine and water, dried over $MgSO_4$ and evaporated, producing the capsules as yellow powder.

Capsule 1. Yield: 50%. ^{1}H NMR (500 MHz, C_5D_5N) δ 12.24 (s, 2H), 11.81 (s, 2H), 11.53 (s, 2H), 10.88 (s, 2H), 10.61 (bs, 2H), 10.28 (s, 2H), 9.15 (d, *J* = 7.5 Hz, 2H), 8.93 (bs, 2H), 8.85 (d, *J* = 8.5 Hz, 2H), 8.78 (s, 1H), 8.77 (d, *J* = 8.5 Hz, 2H), 8.67 (d, *J* = 8.5 Hz, 2H), 8.64 (s, 1H), 8.56 (s, 1H), 8.44 (d, *J* = 8.0 Hz, 2H), 8.42 (s, 1H), 8.30 (d, *J* = 8.0 Hz, 2H), 8.03 (s, 2H), 8.00 (d, *J* = 8.0 Hz, 2H), 7.99 (s, 2H), 7.94 (d, *J* = 7.5 Hz, 2H), 7.84 (d, *J* = 7.5 Hz, 2H), 7.76 (t, *J* = 8.5 Hz, 2H), 7.62 (s, 1H), 7.60 (s, 1H), 7.50 (d, *J* = 7.5 Hz, 2H), 7.41-7.38 (m, 4H), 7.34 (t, *J* = 8.0 Hz, 2H), 7.31 (s, 2H), 7.20 (d, *J* = 7.5 Hz, 2H), 6.84 (d, *J* = 8.0 Hz, 2H), 6.75 (s, 2H), 6.25 (d, *J* = 8.0 Hz, 2H), 4.04-4.02 (m, 6H), 3.64 (bs, 4H), 2.24-2.21 (m, 7H), 1.99-1.94 (m, 3H), 1.88-1.82 (m, 3H), 1.24 (s, 6H), 1.14 (bs, 6H), 1.18 (d, *J* = 6.5 Hz, 12H), 1.13 (d, *J* = 6.5 Hz, 15H), 1.00 (d, *J* = 6.5 Hz, 9H), 0.86 (s, 9H), 0.67 (bs, 9H) ppm. HRMS (ESI+): m/z calcd for $C_{348}H_{335}N_{64}O_{52}S_4$ $[2M+3H]^{3+}$ 2124.4846 found 2124.4932.

Capsule 2. Yield 40%. ^{1}H NMR (500 MHz, $CDCl_3$) δ 11.91 (s, 2H), 11.59 (s, 2H), 11.50 (s, 2H), 11.39 (s, 2H), 10.57 (bs, 2H), 10.29 (s, 2H), 10.07 (s, 2H), 9.59 (s, 2H), 8.90-8.85 (m, 4H), 8.78 (d, *J* = 8.5 Hz, 2H), 8.76 (d, *J* = 8.5 Hz, 2H), 8.56 (s, 2H), 8.41 (dd, *J* = 7.5, 1.0 Hz, 2H), 8.34 (b, 2H), 8.60 (d, *J* = 8.0 Hz, 2H), 7.83 (b, 4H), 7.77 (s, 2H), 7.75 (s, 2H), 7.71 (d, *J* = 8.0 Hz, 2H), 7.57 (b, 1H), 7.48 (b, 1H), 7.43 (d, *J* = 8.0 Hz, 2H), 7.35 (b, 1H), 7.33 (dd, *J* = 7.5, 7.5 Hz, 1H), 7.29 (dd, *J* = 7.5, 1.0 Hz, 2H), 7.20 (s, 2H), 7.18 (d, *J* = 7.5 Hz, 2H), 7.11-7.08 (m, 1H), 7.02-7.00 (m, 1H), 6.97 (d, *J* = 7.5 Hz, 2H), 6.91-6.80 (m, 12H), 6.21 (t, *J* = 7.5 Hz, 2H), 4.21 (bs, 12H), 4.07 (bs, 2H), 3.99 (bs, 2H), 3.81 (bs, 2H), 3.72 (bs, 2H), 3.27 (bs, 2H), 3.12 (bs, 2H), 2.45-2.37 (m, 7H), 2.33-2.23 (m, 9H), 2.17-2.11 (m, 2H), 1.82 (bs, 6H), 1.64-1.55 (m, 4H), 1.26-1.20 (m, 54H), 1.10 (bs, 6H), 1.03-1.01 (m, 12H), 0.75 (bs, 6H), 0.53 (bs, 6H) ppm. HRMS (ESI^+): m/z calcd for $C_{212}H_{215}N_{38}O_{34}S_2$ $[M+3H]^{3+}$ 1300.8585 found 1300.8653; $C_{212}H_{214}N_{38}O_{34}S_2$ $[M+2H]^{2+}$ 1950.7841 found 1950.7950.

2. Comparison of UV-Vis Spectra

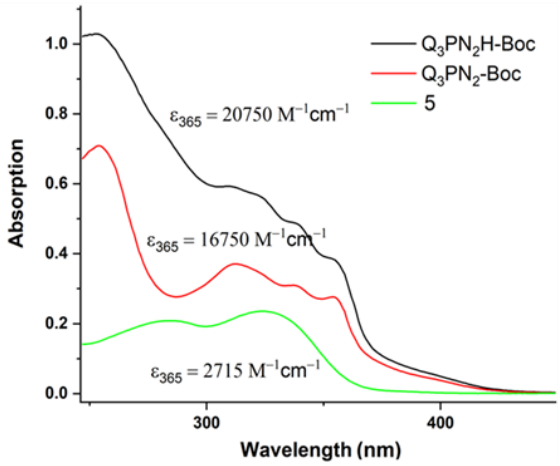

Figure S1. Comparison of UV-Vis spectra of **5** with Boc protected amines **7** and **8** in 5% DMSO in chloroform (at 10^{-5} M).

3. Fatigue test toward 365 nm light irradiation

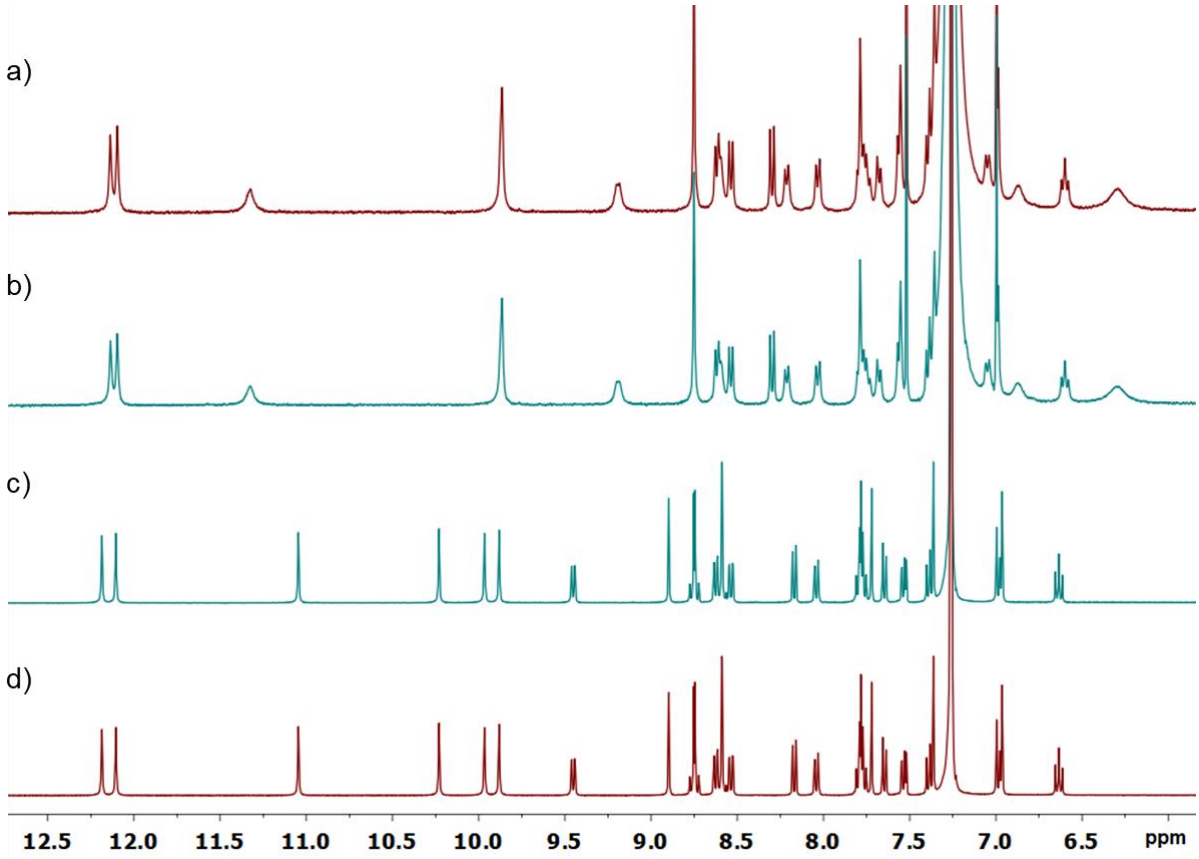

Figure S2. Partial ^{1}H NMR spectra (400 MHz, 298K) of free amine **7** (a) before and (b) after, and Boc-**7** (c) before and (d) after shining 365 nm light for 10 minutes in $CDCl_3$.

4. Concentration dependent studies

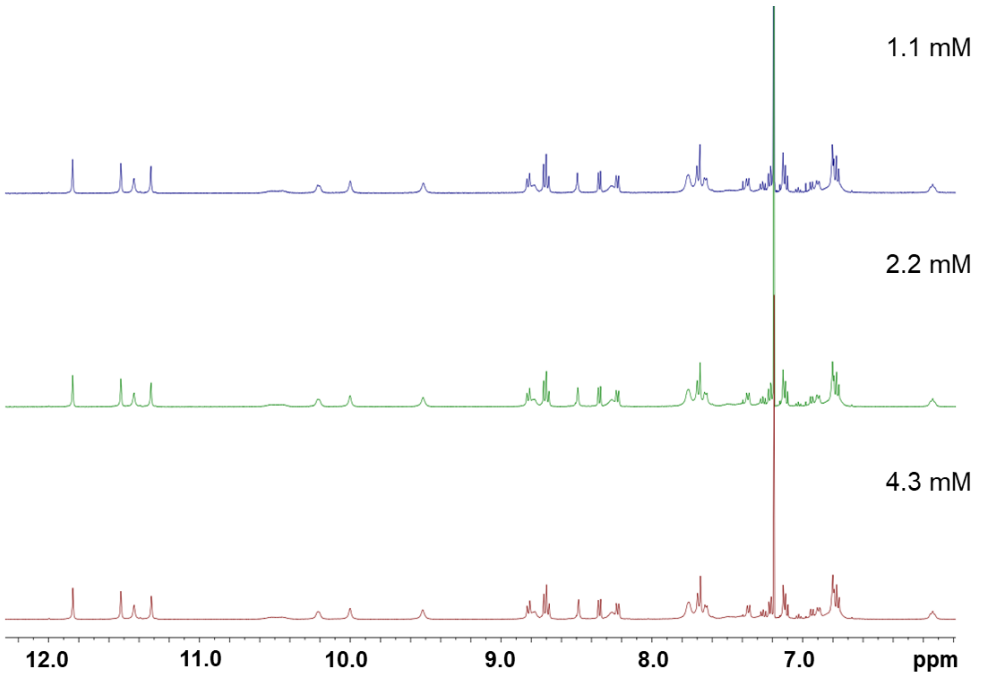

Figure S3. Partial ^{1}H NMR spectra (500 MHz, $CDCl_3$, 298K) of capsule **2º** at different concentrations. The number of signals indicates a symmetrical structure on average, unlike the aggregated from observed in the solid state. The absence of chemical shift dependence of concentration suggests that the molecule is monomeric.

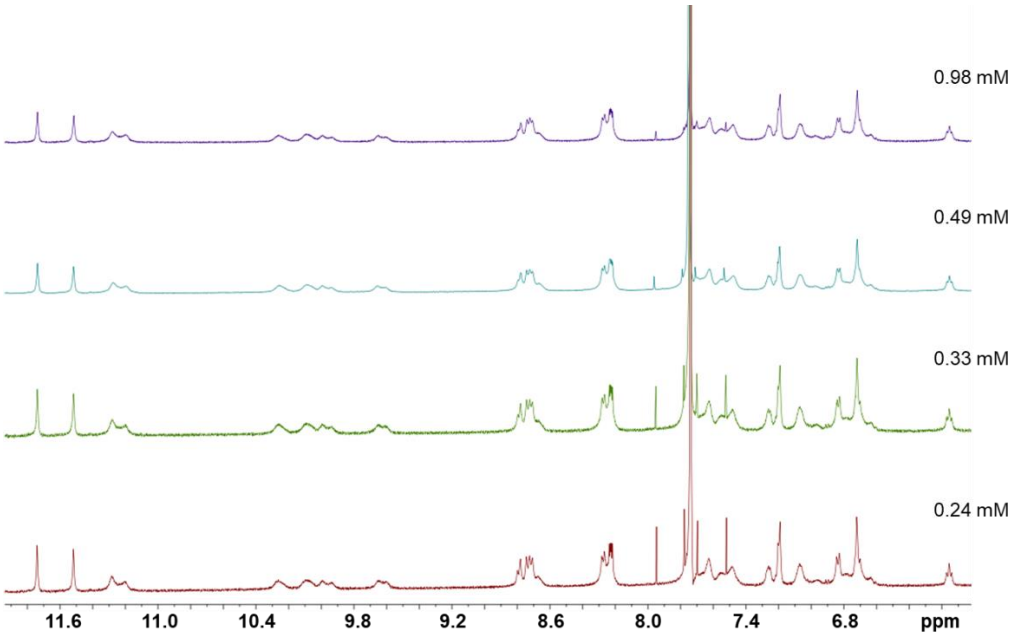

Figure S4. Partial ^{1}H NMR spectra (500 MHz, $CDCl_3$, 298K) of capsule **2º** at different concentrations in 30/70 DMSO-d_6:$CDCl_3$ vol/vol. The number of signals indicates a symmetrical structure on average, unlike the aggregated from observed in the solid state. The absence of chemical shift dependence of concentration suggests that the molecule is monomeric.

5. Photoswitching of empty hosts

5.1 Procedures

Irradiation was performed with a CoolLED pE excitation system. Freshly distilled (over CaH2) chloroform or toluene, and DMSO (as received) were used to prepare the solution of the capsules. 2 mL of the stock solution was placed in a 1 cm quartz cuvette and oxygen was removed through gentle bubbling on nitrogen for 10 minutes. The cuvette was then capped and irradiation was performed by placing the tube (the light source) in front of the cell window, with continuous stirring (small magnetic stir bar). Switching between the open and the closed form was achieved by shining a 365 nm (2-3 min) or >450 nm (3 min) light source. After each irradiation step, the cell was immediately transferred to the UV-Vis instrument and the spectrum was recorded. For the concentration of each experiment, see the Figure captions.

NMR Studies: chloroform-d was passed through basic alumina in order to neutralize and then 570 μL of it was transfer into a quartz NMR tube which contains the solid capsules. Thereafter, 30 μL of DMSO-d6 was added to adjust the solvent ratio to 95 to 5 (vol/vol). Solutions were bubbled with slow stream of N_2 for 5 min prior to any experiment. Irradiation was performed by placing the irradiation tube close (with in 1 cm distance) to the NMR tube with vigorous stirring. Note: If the solution does not diffuse properly please shake the tube manually with a certain time interval (2-3 min), in order to reach the PSS typically 10 min irradiation was performed

CD Studies: preparation of stock solutions and irradiation were performed as mentioned in the UV-Vis studies. After placing in the CD instrument the solutions were equilibrated for 5 min prior to the data collection in order to reach the desired temperature (273K).

5.2 NMR Studies

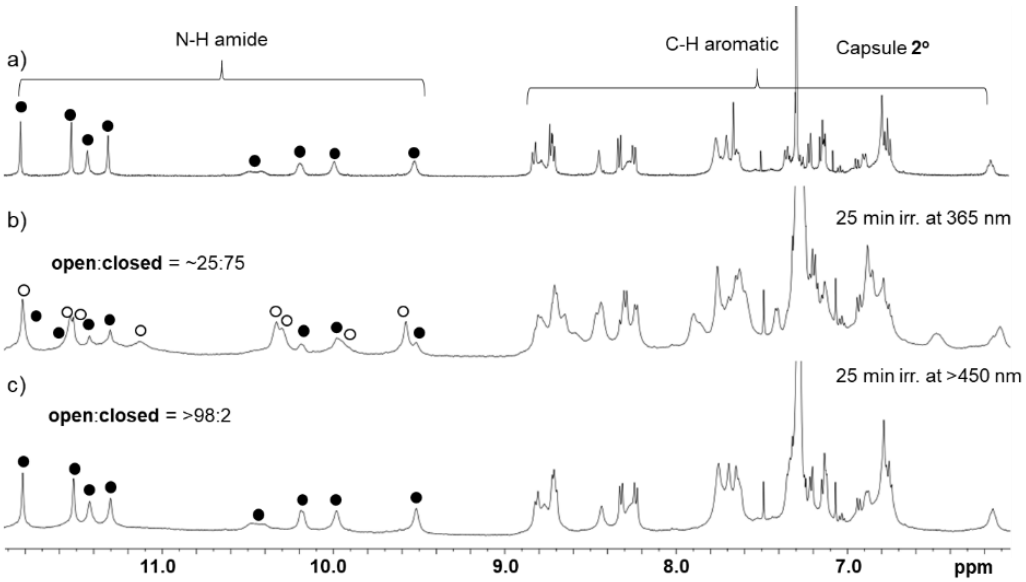

Figure S5. Partial ^{1}H NMR spectra (500 MHz, 298K, $CDCl_3$/DMSO-d_6 (95:5) at [**2º**] = 0.82 mM) of a) capsule **2º** (amide protons are depicted in black circles); b) after irradiation with 365 nm light (amide protons of the **2ᶜ** are depicted in open circles); c) after irradiation with >450 nm light. The presence of a single set of signals for both **2º** and **2ᶜ** is consistent with the presence of a single diasteromeric conformer in which the two Q_3PN_2H segments either have same PP/MM or opposite PM handedness. The crystal structure of **2º** suggest that, for **2º**, this species is the PM conformer.

5.3 UV-Vis studies

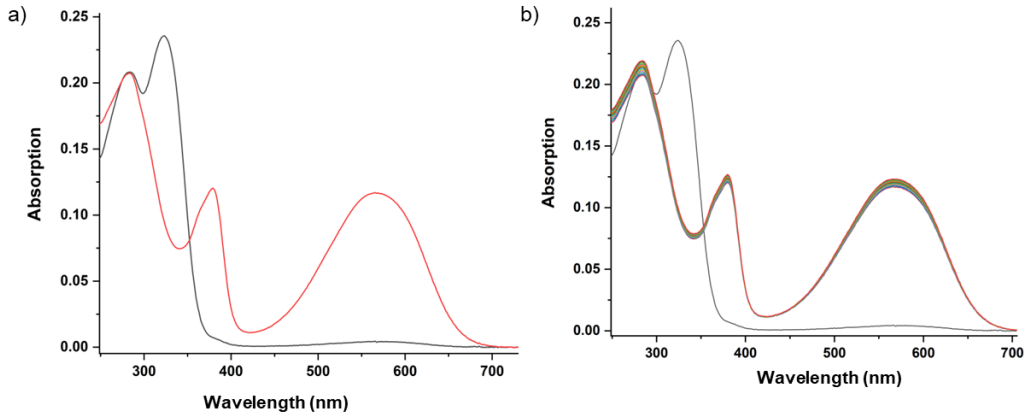

Figure S6. UV-Vis spectra (5% DMSO in chloroform at 1.2×10^{-5} M) of a) light-induced switching (black and red traces are corresponding to **5^{o}** and **5^{c}**, respectively) and b) thermal stability studies over the period of 1h, suggesting that **5^{c}** is thermally stable at room temperature over that period.

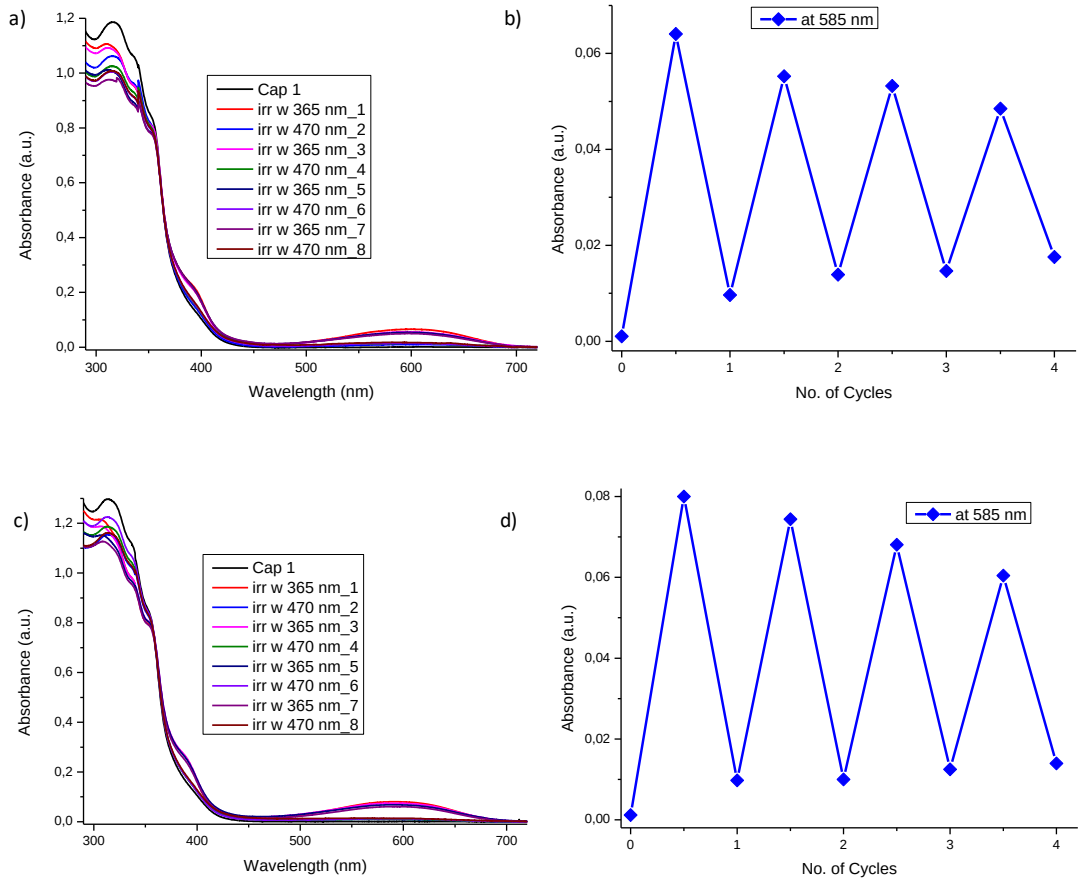

Figure S7. a) UV-Vis spectra of capsule **1** depicting reversible switching upon irradiation with λ = 365 nm and λ > 450 nm light in chloroform/DMSO (95:5) at [**1^{o}**] = 10^{-5} M. b) Change in absorption spectra monitored at 585 nm upon reversible light irradiation, depicting the reversibility of switching and suggesting some fatigue upon prolonged exposure to light. c) and

d) show the same experiment performed in toluene/DMSO (95:5). Fatigue is lower in this solvent. Mass spectrometric analysis of the samples after irradiation showed no indication of masses other than that of **1**, suggesting that fatigue arrises from purely intramolecular processes.[S4]

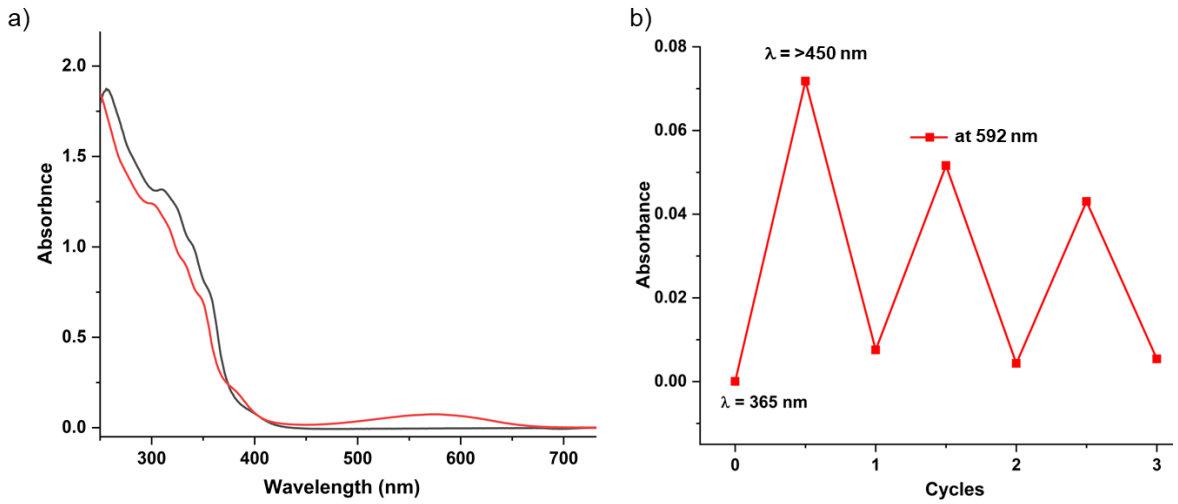

Figure S8. a) UV-Vis spectra of capsule **2** before (black trace) and after (red trace) irradiation with 365 nm light in chloroform/DMSO (95:5) at [**2^{o}**] = 10^{-5} M. b) Change in absorption spectra monitored at 592 nm upon reversible light irradiation, depicting the reversibility of switching and suggesting some fatigue upon prolonged exposure to light. In this experiment, oxygen was not removed and fatigue is more significant.

6. Binding studies

6.1 Procedures

Circular Dichroism (CD) measurements and titrations: CD spectra were recorded on a Jasco J-815 spectropolarimeter at 293 K. Fructose solutions were prepared in DMSO and allowed to equilibrate overnight prior to use. For **2^{o}**, it was found that the onset of CD signals due to helix handedness induction by a fructose guest was slow (Figure S9). Since **2^{o}** is thermodynamically stable, stock solutions were prepared in the presence of different amounts of fructose and equilibrated in parallel for 5h prior to data collection. To assess binding with **2^{c}**, the 75/25 **2^{c}/2^{o}** PSS was generated by irradiating a solution of solution of **2^{o}** with 365 nm light (see corresponding experimental section) prior to titration. For the titrations, samples of the PSS solution were taken in a 1 cm cuvette (2 mL) and the sugar solution was added. Final ratio of the solvent (chloroform to DMSO) was adjusted by adding pure chloroform to the mixture. Cuvettes were then placed in the spectropolarimeter cell holder with temperature control (20°C). The onset of CD bands was found to be somewhat faster than with **2^{o}**, possibly due to faster helix reversal in **2^{c}**. To limit possible thermal reversal of **2^{c}** into **2^{o}**, CD spectra were recorded as soon as they were found not to change anymore. Changes in ellipticity were analysed using a 1:1 binding isotherm for both **2^{o}** and **2^{c}** using the HypSpec 2014 program. The data (entire spectra, i.e. not simple monitoring at one wavelength) of two titrations, one of **2^{o}** and one of the PSS, were fitted simultaneously to extract the K_a value for each equilibrium

consistent with both data sets. This was performed first with D-fructose (Figure 3a-3d), and then repeated with L-fructose (Figure S10-S11), yielding similar results.

NMR titration: Fructose solutions were prepared in DMSO-d_6 and allowed to equilibrate overnight prior to use. Stock solutions of capsule **2º** were prepared in a chloroform-d and DMSO-d_6 mixture (95:5) prior to measurements. Aliquot of the fructose solution were added and the final solvent ratio was adjusted by adding pure chloroform-d. The mixtures were shaken thoroughly and equilibrated prior to each data collection.

6.2 CD Titrations

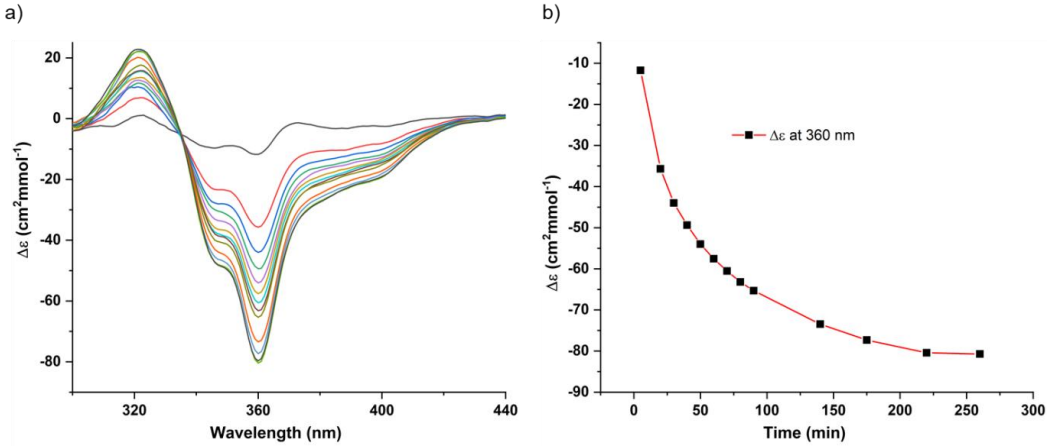

Figure S9. CD spectra (at 293K) for monitoring the kinetics of D-fructose binding by **2º** in $CHCl_3$/DMSO (95:5) at [**2º**] = 10^{-5} M. The solution was treated with 25 equiv. of sugar and CD data were recorded over time. b) Plot of change in the Δε with respect to time. Note that this experiment does not tell about the inherent helix reversal rate of **2º**, but its reversal rate when saturated with fructose. One can envisage that fructose initially binds both *P* and *M* conformers and that binding slows down helix reversal.

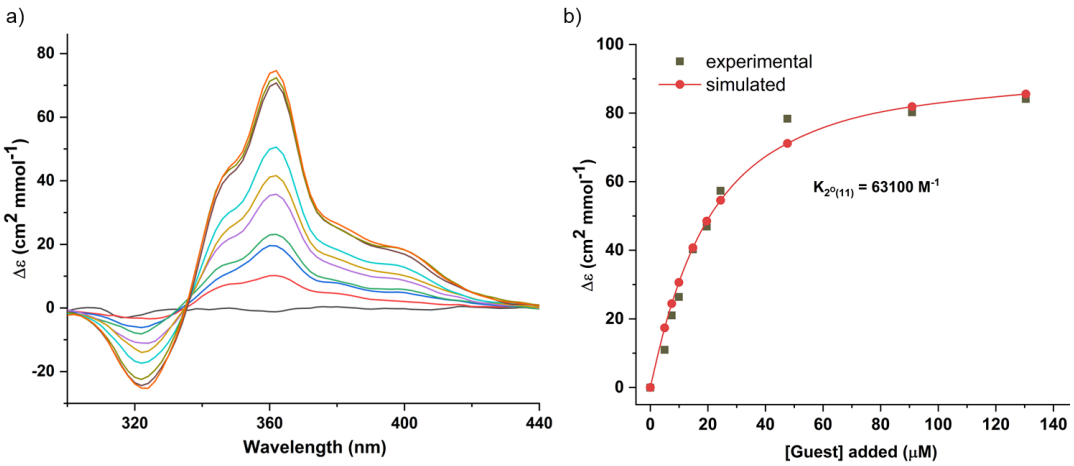

Figure S10. a) CD spectra (at 293K) for the binding of L-fructose by **2º** in $CHCl_3$/DMSO (95:5) at $[\mathbf{2^o}]_{initial}$ = 10^{-5} M. b) Curve fitting of binding isotherm using 1:1 binding model. This experiment mirrors that shown in Fig. 3a,b. The difference between binding constants reflect experimental variations.

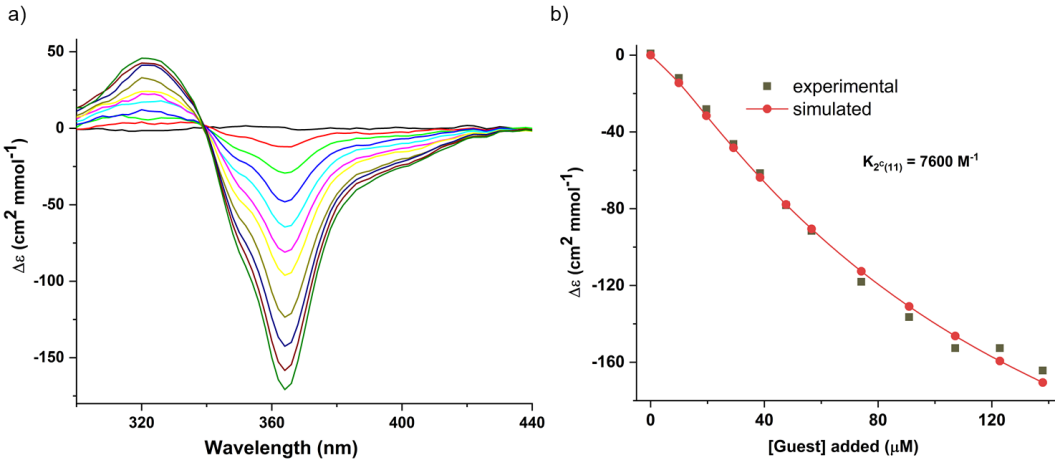

Figure S11. a) CD spectra recorded at 293K for the binding of L-fructose by **2^{c}** in $CHCl_3$/DMSO (95:5) at $[\mathbf{2^{o}}]_{initial} = 10^{-5}$ M. b) Curve fitting of binding isotherm using 1:1 binding model taking into account the presence of 25% 2^{o}. This experiment mirrors that shown in Fig. 3c,d. The difference between binding constants reflect experimental variations.

6.3 NMR Titrations

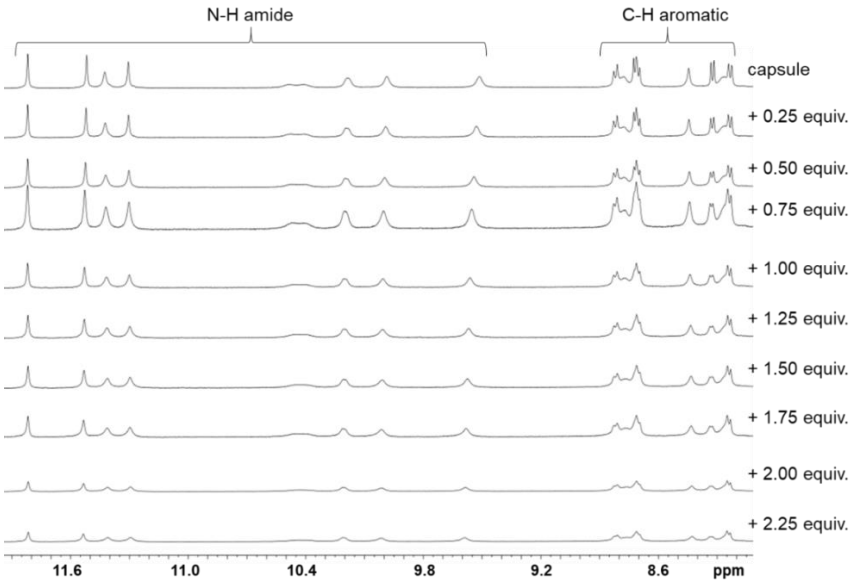

Figure S12. Part of the ^{1}H NMR spectra (500 MHz, 298K) of capsule **2^{o}** in the presence of different amounts of D-fructose in $CDCl_3$/DMSO-d_6 (95:5) at $[\mathbf{2^{o}}]_{initial}$ = 0.86 mM. Continuous chemical shifts variations of amide protons are the result of fast exchange between **2^{o}** and **2^{o}**⊃D-fructose on the NMR times scale. The NMR lines broaden because fructose exists in different α/β and pyranose/furanose configurations which each may engage in more than one binding complex geometry. The broadening of the lines is probably the reason why different sets of signals are not observed for MM-**2**⊂fructose and PM-**2**⊂fructose, which must equilibrate slowly on the NMR time scale.

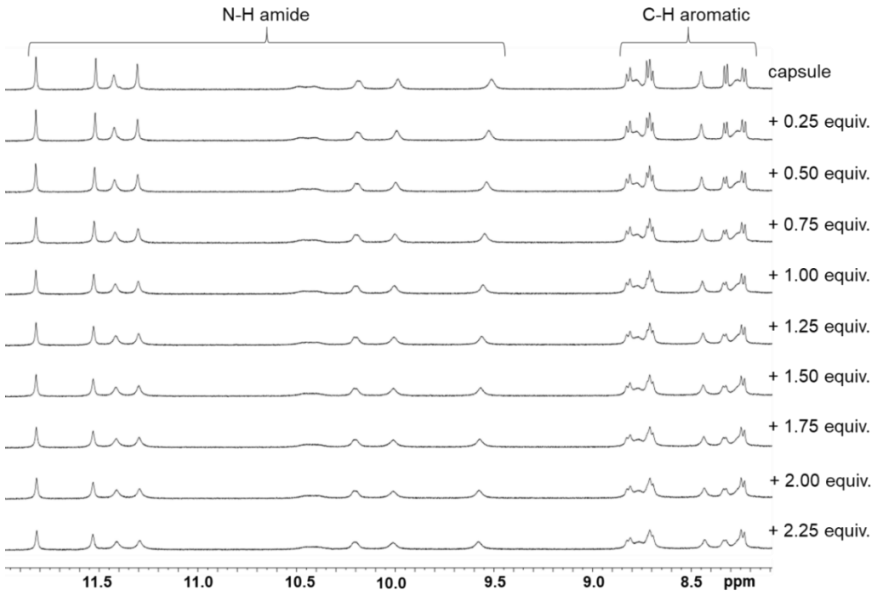

Figure S13. Part of the ^{1}H NMR spectra (500 MHz, 298K) of capsule **2º** in the presence of different amounts of L-fructose in $CDCl_3$/DMSO-d_6 (95:5) at $[\mathbf{2^o}]_{initial}$ = 0.82 mM. See Figure above for comments.

6.4 Temperature Dependent Studies

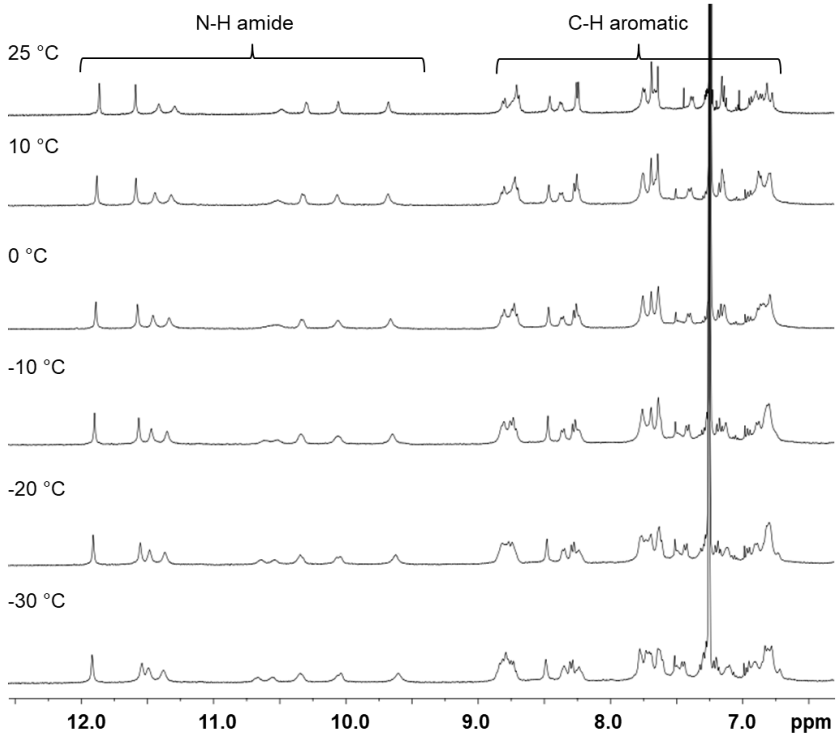

Figure S14. Part of the ^{1}H NMR spectra (400 MHz, $CDCl_3/CD_3OH$ (95:5)) of **2º**⊃D-fructose (0.5 equiv.) at different temperatures, $[\mathbf{2^o}]_{initial}$ = 1.10 mM. The spectra depict chemical shifts variations of the amide protons and splitting of the hydrazodicarboxylate protons near 10.5 ppm. No indication of a slow exchange on the NMR time scale was observed even at low temperature.

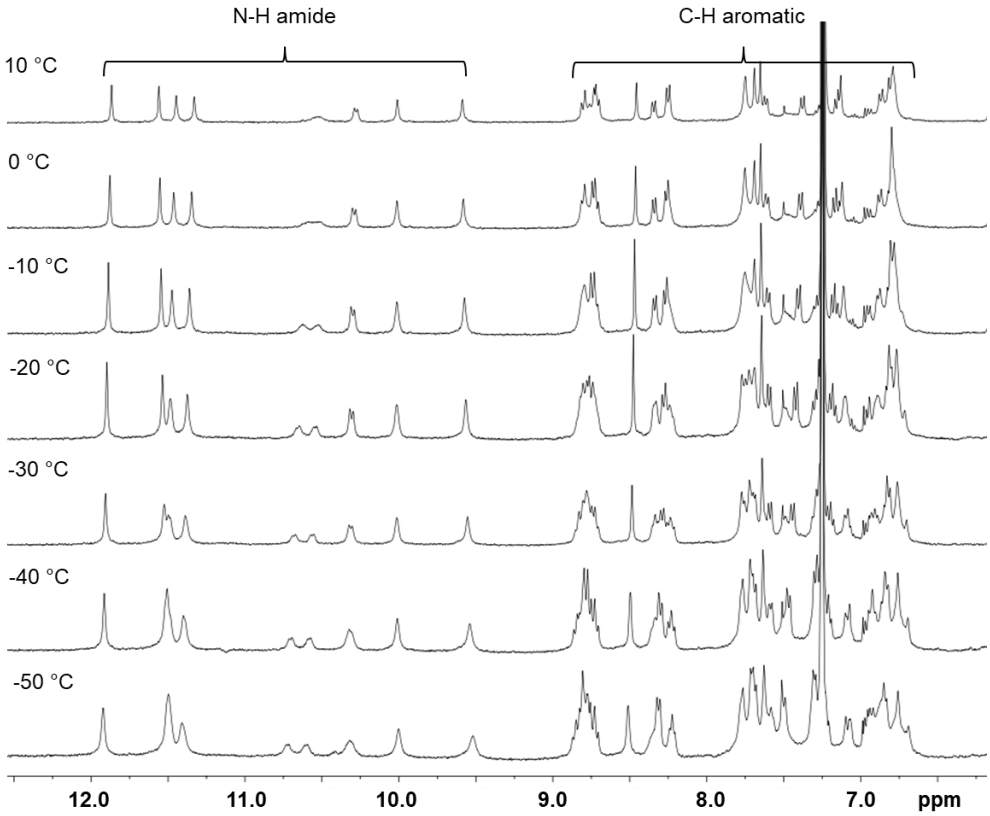

Figure S15. Partial ^{1}H NMR spectra (400 MHz, $CDCl_3/CD_3OH$ (95:5)) of **2º**⊃D-fructose (1.0 equiv.) at different temperatures, $[\mathbf{2^o}]_{initial}$ = 0.98 mM. The spectra depict similar results as observed in Figure S16.

7. Switching of host-guest complex

7.1 Circular Dichroism Studies

Procedure: All the experiments were performed with an initial concentration of 10 μM. Sugar solutions were equilibrated in DMSO overnight prior to use. Solutions of **2^{o}**⊃D- or L-fructose (25 equiv.) in 5/95 DMSO:chloroform vol/vol solvent mixture were equilibrated for 5h prior to data collection. Light-induced reversible switching between **2^{o}** and **2^{c}** was accomplished using 365 nm and >450 nm light irradiation. In each step the resulting solutions were equilibrated for 30 min prior to data collection.

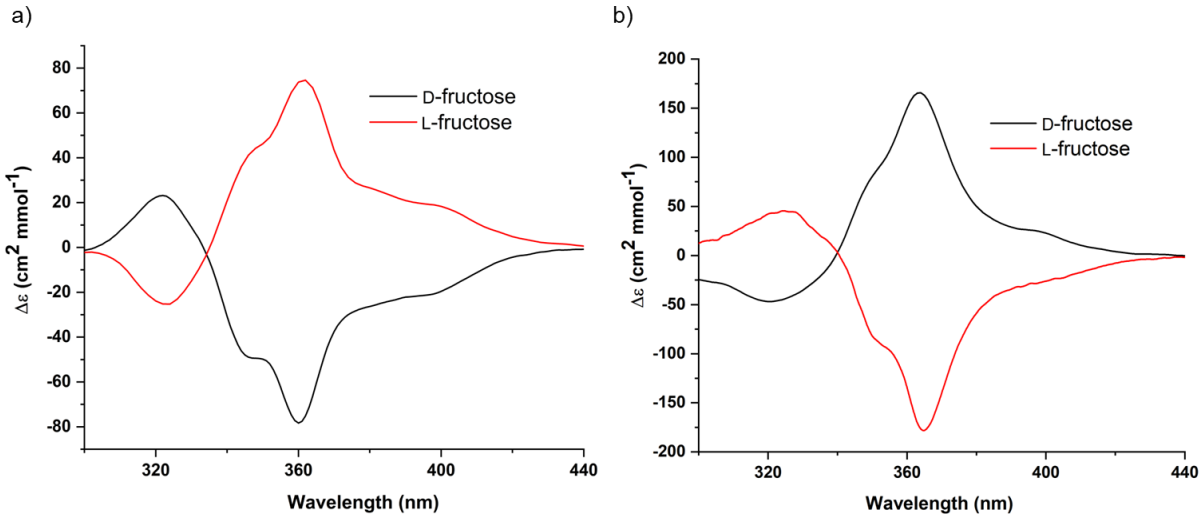

Figure S16. CD spectra (in 5% DMSO in chloroform at 10^{-5} M, 293K) in the presence of D- and L- fructose of a) **2^{o}** and b) **2^{c}** (PSS mixture obtained by irradiation prior to sugar addition).

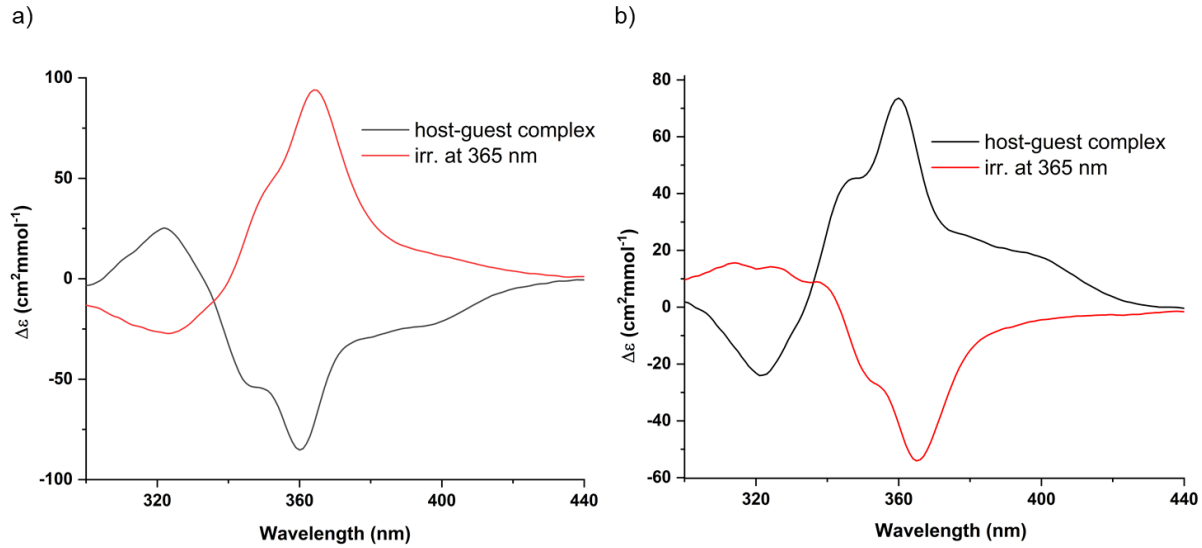

Figure S17. CD spectra (in 5% DMSO in chloroform at 10^{-5} M, 293K) for in-situ switching of helical chirality of capsule **2** in presence of a) D-fructose, and b) L-fructose, upon reversible photoirradiation. In situ switching was performed starting with the **2^{o}**⊃D-fructose or **2^{o}**⊃L-fructose.

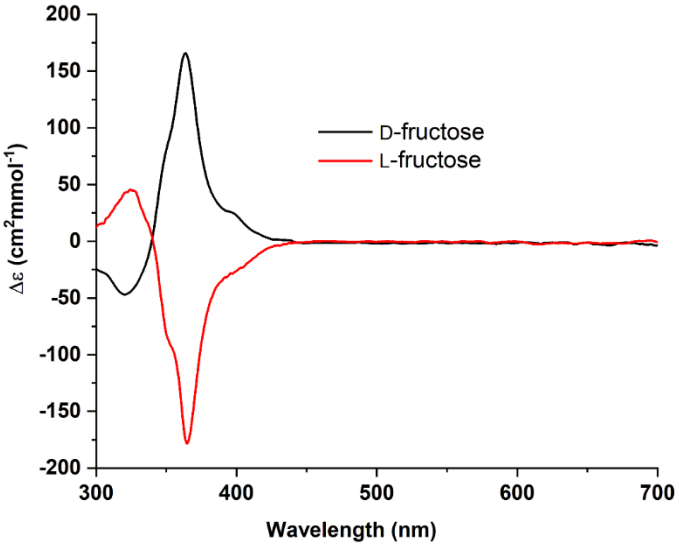

Figure S18. CD spectra (in 5% DMSO in chloroform at 10^{-5} M, 293K) of a mixture of **2** and fructose (25 equiv.) after UV irradiation at 365 nm. The region between 500 and 700 nm shows not band that would have belonged to the closed form of the switch and been indicative of a transfer of chirality from the sugar to the switch absolute configuration.

7.2 NMR Studies

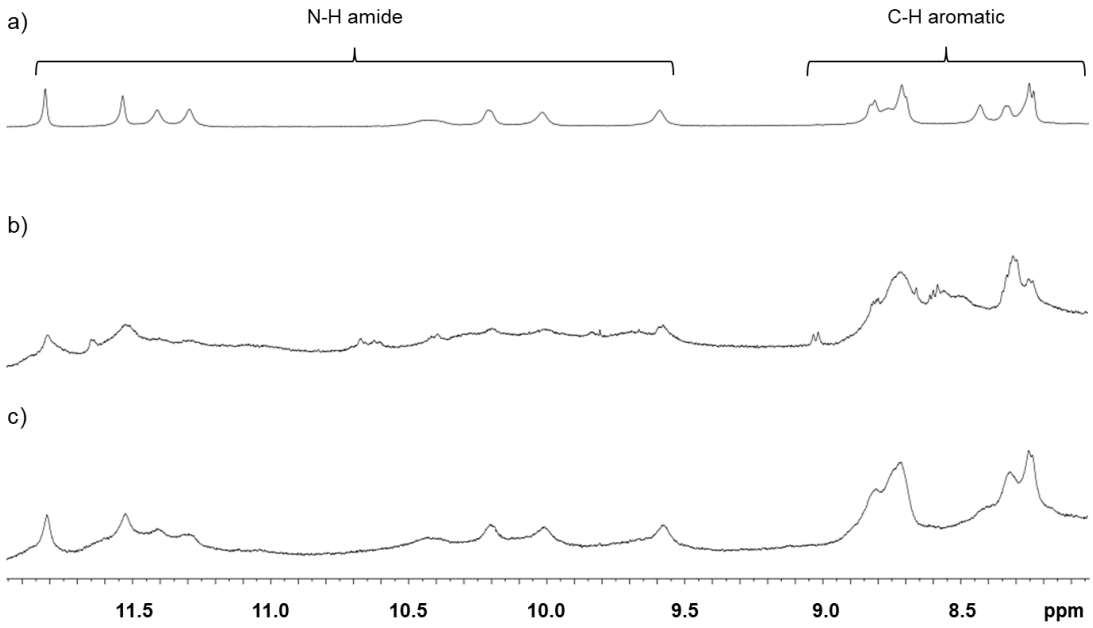

Figure S19. Part of the ^{1}H NMR spectra (500 MHz, 298K, in $CDCl_3$/DMSO-d_6 (95:5)) of a) **2º**⊃D-fructose (2.25 equiv.); b) after irradiation with 365 nm light for 25 minutes; c) obtained after irradiation of the same solution with >450 nm light for 10 min at $[\mathbf{2^o}]_{initial}$ = 0.68 mM.

8. Molecular Modelling

Molecular modelling calculations were performed using MacroModel (Schrödinger Release 2019-2: MacroModel, Schrödinger, LLC, New York, NY, 2019) using the MMFFs force-field as implemented in this software. Energy minimized structures were obtained using 2500 steps of Truncated Newton Conjugate Gradient (TNCG) under vacuum. The modelling of the host-guest complexes were performed without any constrain. All the structures are presented without the side chain.

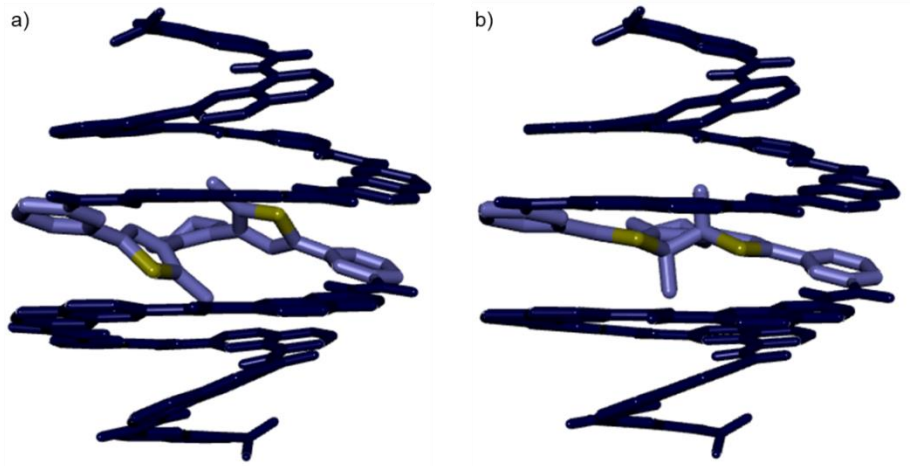

Figure S20. Energy minimized models (MacroModel, MMFFs force field) of a) **1º** and b) **1ᶜ**, suggesting helical conformation would not change upon ring closing. Additionally, the methyl groups protrude inside the cavity albeit at different orientations.

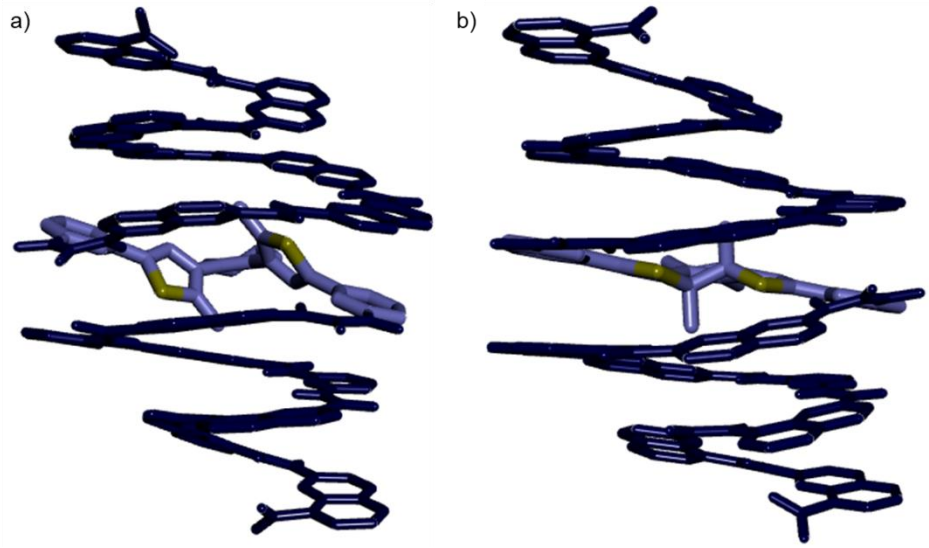

Figure S21. Energy minimized models (MacroModel, MMFFs force field) of a) **2º** and b) **2ᶜ**. Structural information alike to the capsule **1** were found.

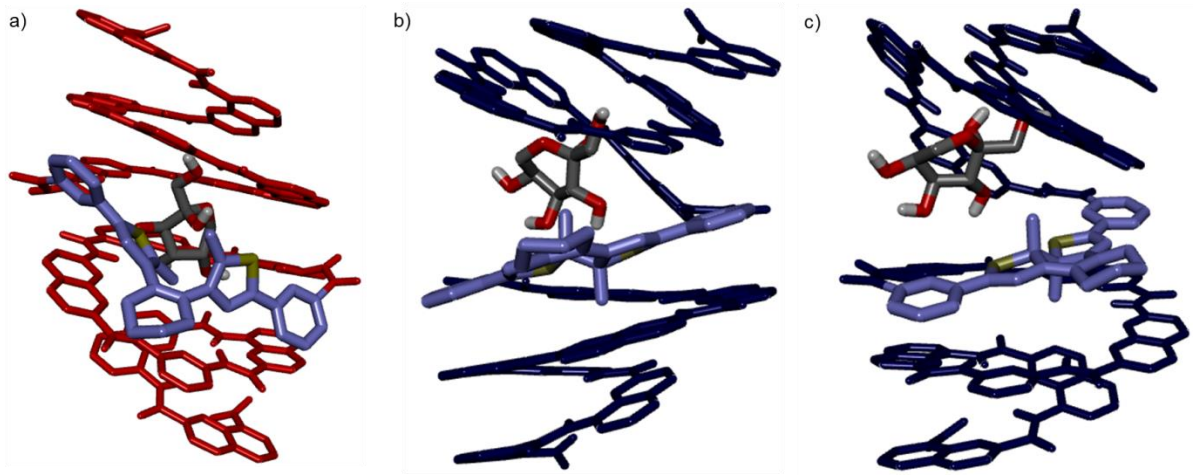

Figure S22. Energy minimized models (MacroModel, MMFFs force field) of a) **2º**⊃α-D-fructopyranose (the capsule completely secludes the guest) and b-c) different views of **2ᶜ**⊃α-D-fructopyranose (the guest moves to one hemi-capsule in order to avoid interference from the methyl group).

9. Single crystal structures

Crystallizing conditions:

1º: Single crystals were obtained upon vapour diffusion of methanol in to a solution of **1º** in pyridine. Co-crystals of **1º** and **1ᶜ** overlapped in a 70:30 ratio were obtained.

1º-$MgCl_2$: Layer diffusion of n-hexane in to a solution of **1º** in dichloromethane resulted in single crystals suitable for X-ray diffraction.

2º: Solution of **2º** in 1:4 DMSO and chloroform solvent mixture was prepared and followed by the layer diffusion of n-hexane and diethylether led to single crystals suitable for X-ray diffraction.

Table 1. Crystalographic data for the capsules **1** and **2**

Structures	**1º/1ᶜ** cocrystal	**1º**-$MgCl_2$	**2º**
CCDC	2032748	2032749	2032750
net formula	$C_{176}H_{176}N_{32}O_{28}S_2$	$C_{199}H_{226}Cl_4F_6MgN_{32}O_{27}PS_2$	$C_{430}H_{458}N_{80}O_{74}S_9$
M_r/*g mol*$^{-1}$	3251.60	2032749	8219.28
crystal size/mm	0.1x0.1x0.1	0.1x0.1x0.1	0.1x0.1x0.1
crystal system	Monoclinic	Triclinic	Monoclinic
space group	P2(1)/c	P-1	P2(1)/c
a/Å	19.6936(2)	19.9465(7)	39.9797(6)
b/Å	38.3273(3)	20.6535(6)	39.0226(4)
c/Å	27.2035(3)	29.5300(9)	35.4973(5)
α/°	90	70.680(3)	90
β/°	97.4660(10)	82.045(3)	110.728(2)
γ/°	90	68.219(3)	90
V/Å^3	20359.2(3)	10659.0(7)	51795.1(14)
Z	4	2	4
calc. density/g cm^{-3}	1.061	1.207	1.054
μ/*mm*$^{-1}$	0.784	1.376	0.927
refls. Measured	148080	140060	259363
R_{int}	0.0590	0.0771	0.0418
θ max °	73.420	69.872	55.572
observed refls.	40202	38563	65674
Parameters	2280	2512	5382
Restraints	450	2179	195
R(Fobs)	0.0852	0.0909	0.1189
$R_w(F^2)$	0.2410	0.2589	0.3485
S	1.029	1.046	1.391
max. electr. dens./eÅ^{-3}	1.28	1.21	1.33
min. electr. dens./eÅ^{-3}	-0.6	-1.7	-0.96

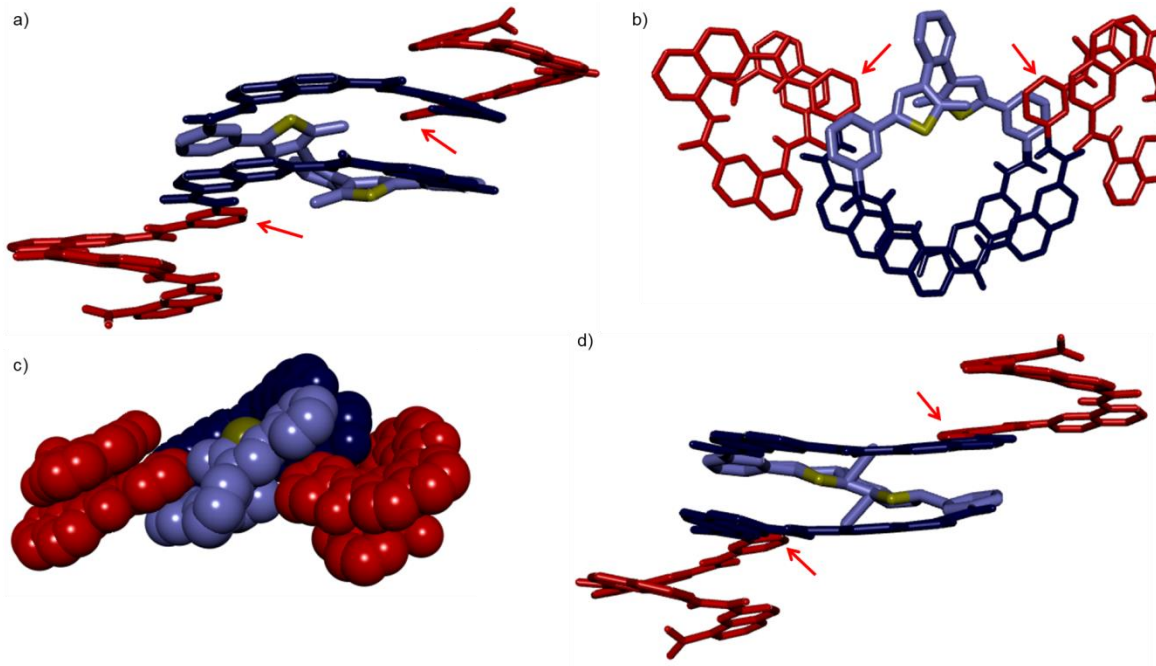

Figure S23. a-d) Crystal structures of the capsule **1** presented in different forms. a) Side and b) top views in stick, and c) space filling representations of **1^{o}**. d) Side view of the **1^{c}**. Co-crystallization indicates a minute structural change would occur upon switching from open to closed form and also crystal to crystal is possible in a big molecule like capsule **1**.

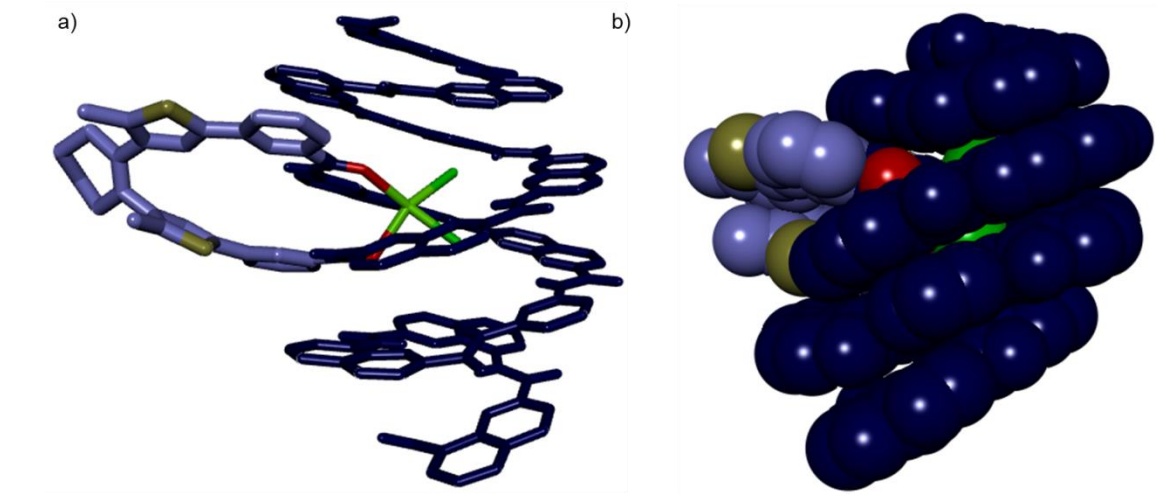

Figure S24. a) Stick and b) space filling representations of crystal structure of the **1^{o}**-$MgCl_2$. The ion coordinates to the carbonyl oxygen of the **S** unit and placed the two thiophene rings in an unfavourable situation for ring closure.

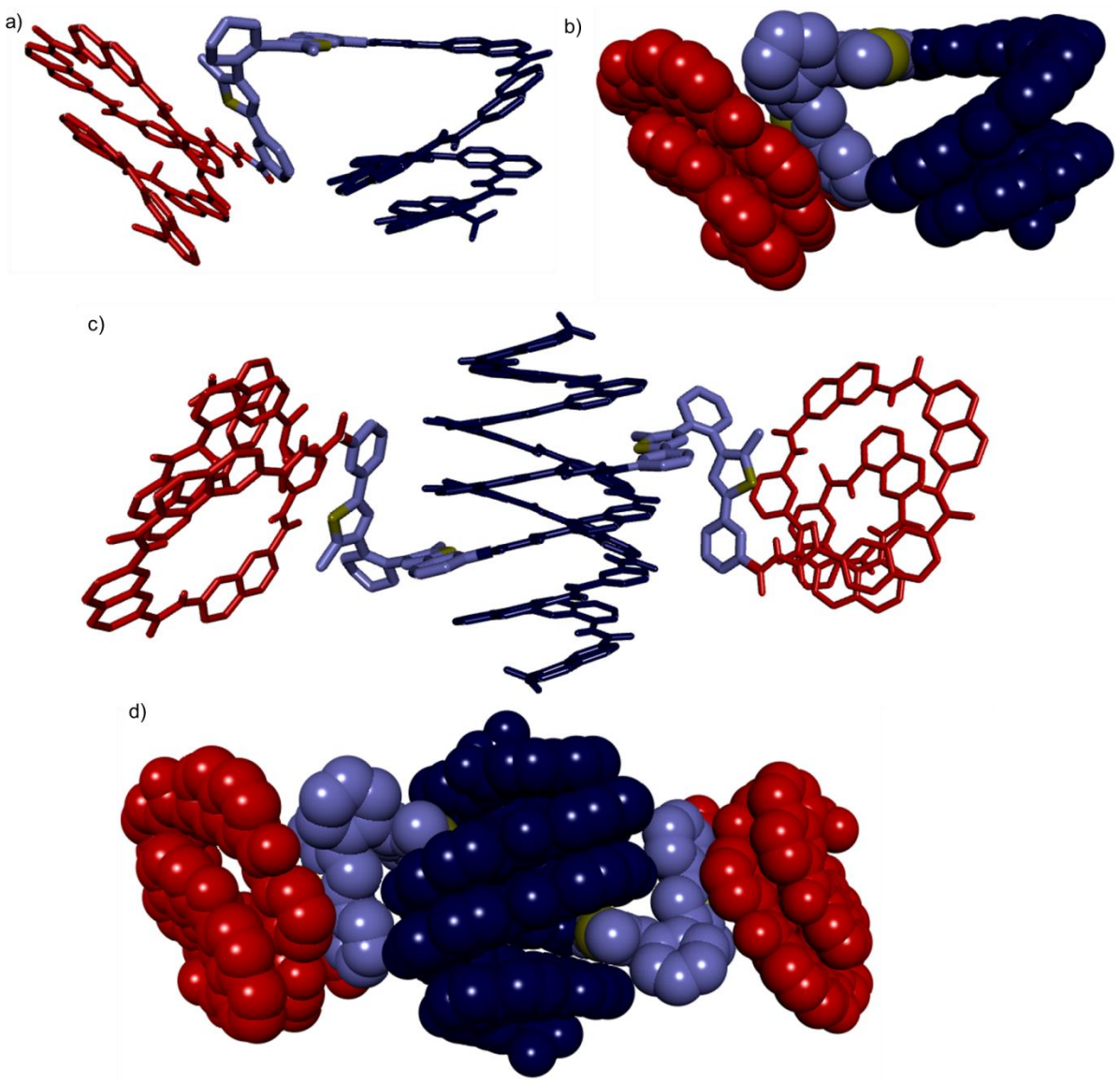

Figure S25. Crystal structure of **2º** in different views. a) Stick and b) space filling representations as a single helix. c) Stick and d) space filling representations of the double helix. In the crystal lattice one of the **Q_3PN_2H** intertwined with that of a neighbouring molecule producing a double helix and each of these segments positioned as two independent hemi-capsules.

10. NMR spectra

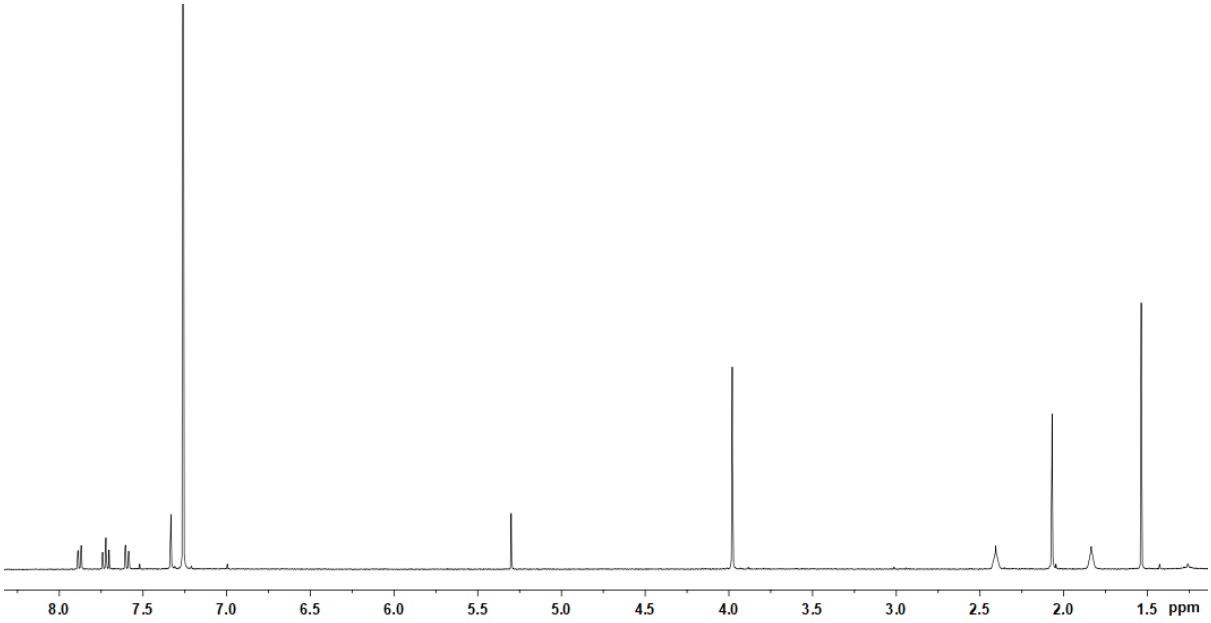

Figure S26. ^{1}H NMR spectra (400 MHz, 298K, $CDCl_3$) of compound **5**.

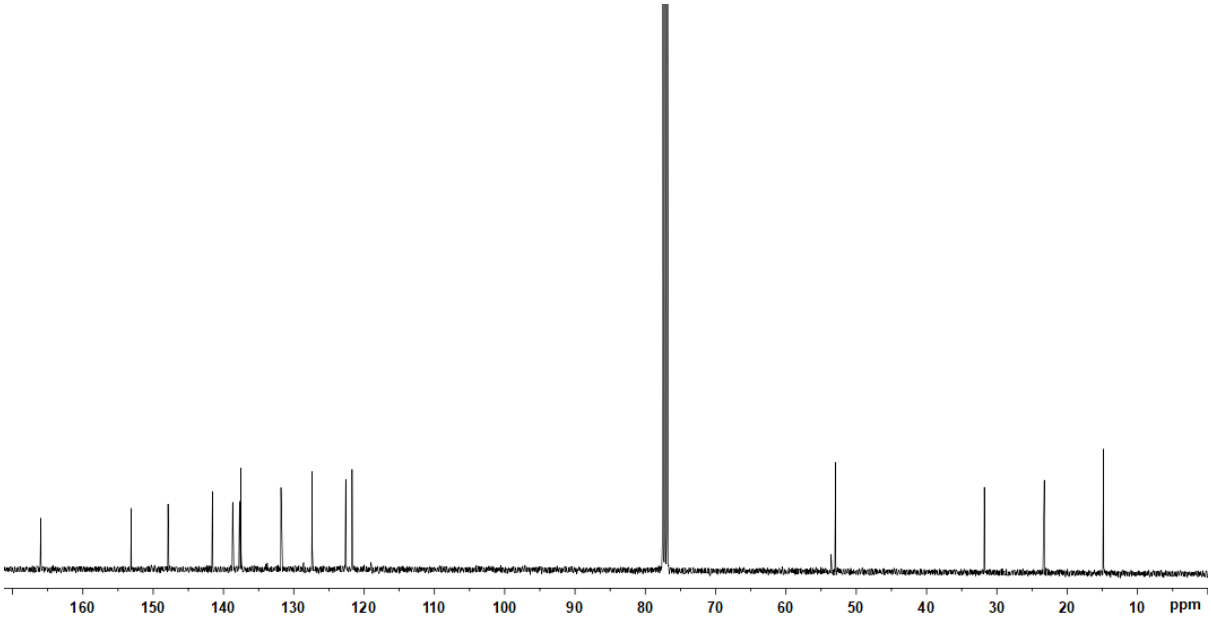

Figure S27. ^{13}C NMR spectra (100 MHz, 298K, $CDCl_3$) of compound **5**.

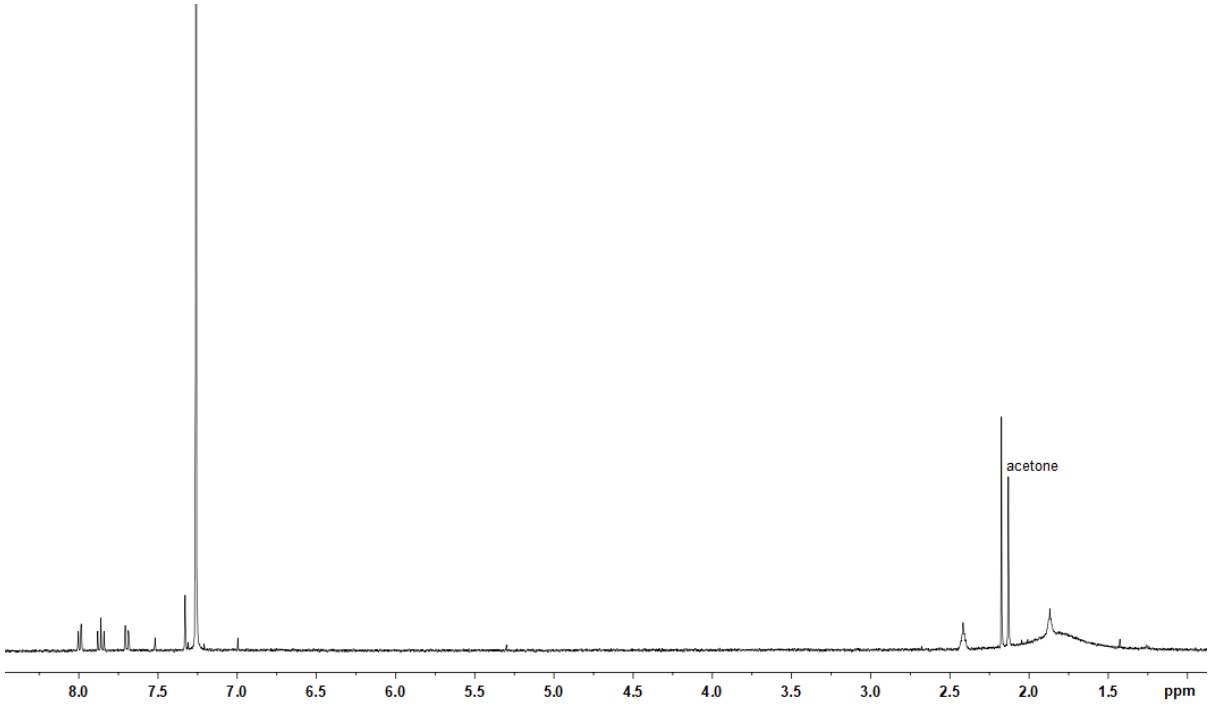

Figure S28. ^{1}H NMR spectra (400 MHz, 298K, $CDCl_3$) of compound **6**.

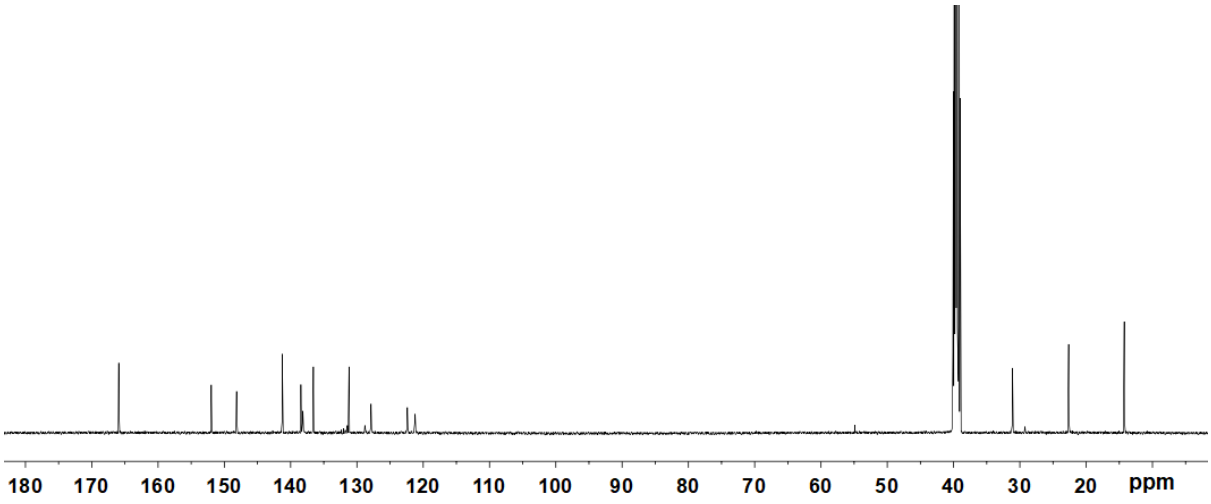

Figure S29. ^{13}C NMR spectra (100 MHz, 298K, DMSO-d_6) of compound **6**.

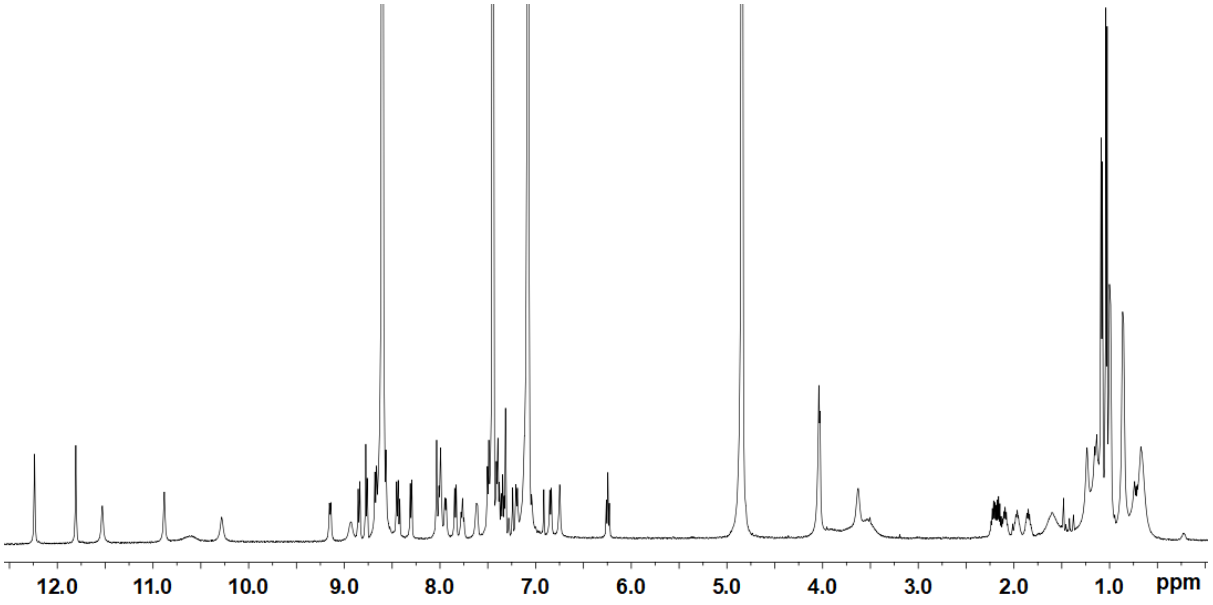

Figure S30. ^{1}H NMR spectra (500 MHz, 298K, Pyridine-d_5) of Capsule **1**.

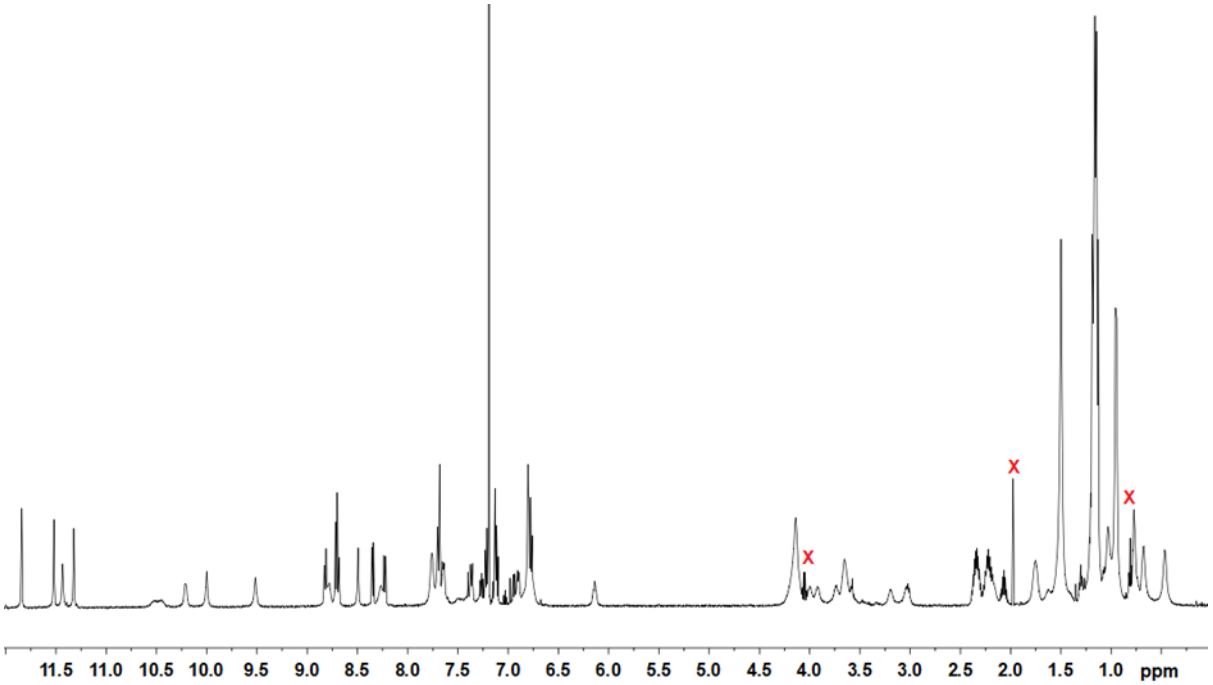

Figure S31. ^{1}H NMR spectra (500 MHz, 298K, $CDCl_3$) of capsule **2**. Signals assigned with red crosses are corresponding to ethyl acetate.

11. HRMS Spectra

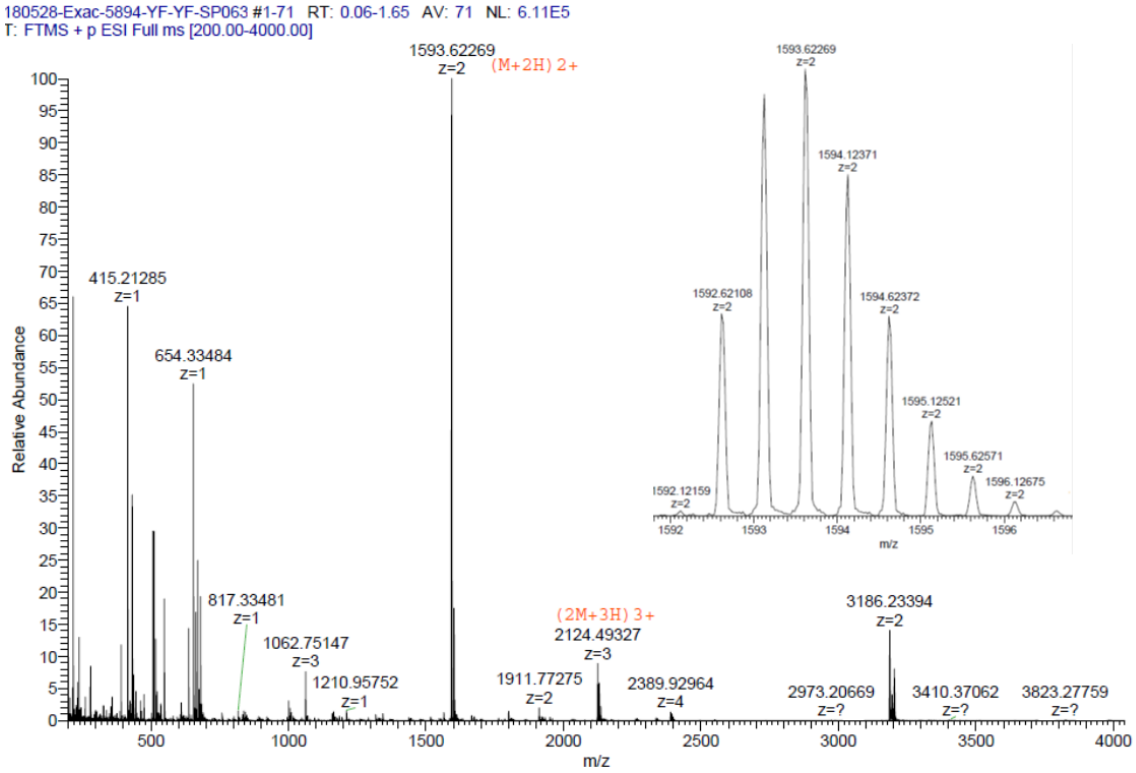

Figure S32. HRMS spectrum of capsule **1**.

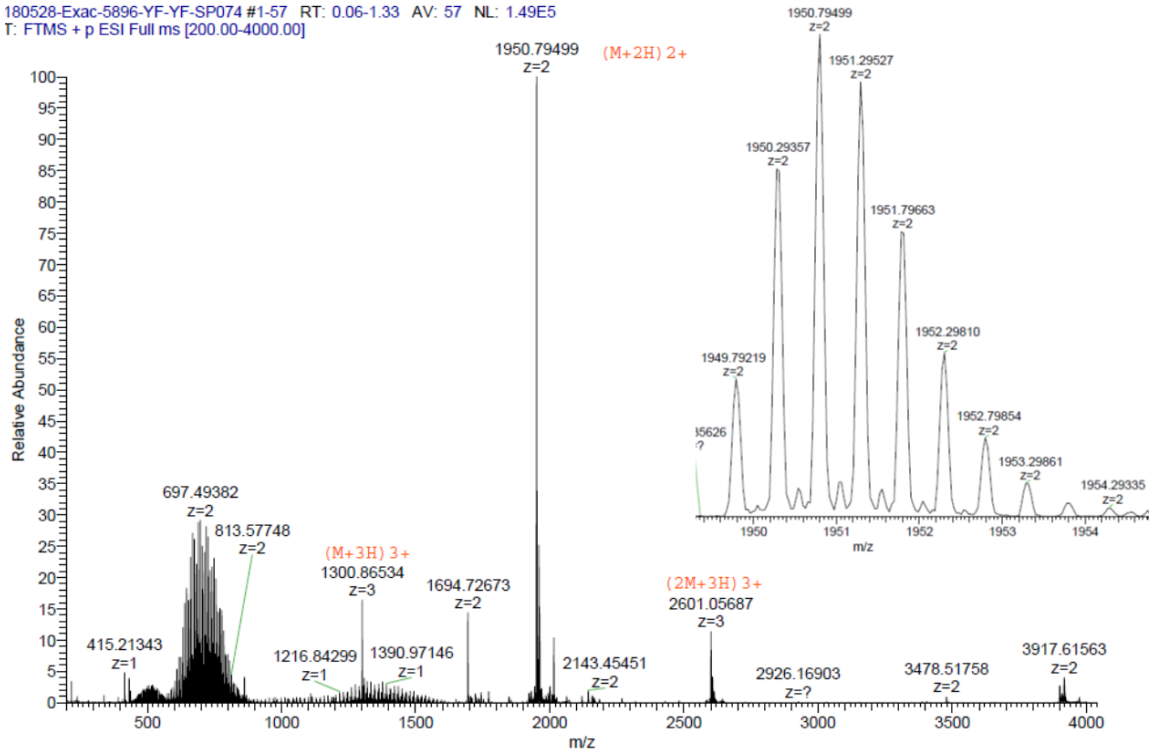

Figure S33. HRMS spectrum of capsule **2**.

12. References

S1. L. N. Lucas, J. J. D. de Jong, J. H. van Esch, R. M. Kellogg and B. L. Feringa, Eur. *J. Org. Chem*., 2003, 155–166.

S2. Y. Ferrand, A. M. Kendhale, B. Kauffmann, A. Grélard, C. Marie, V. Blot, M. Pipelier, D. Dubreuil, and I. Huc, *J. Am. Chem. Soc*., 2010, **132**, 7858–7859.

S3. N. Chandramouli, Y. Ferrand, G. Lautrette, B. Kauffmann, C. D.Mackereth, M. Laguerre, D. Dubreuil and I. Huc, *Nat. Chem*., 2015, **7**, 334–341.

S4. M. Irie, T. Lifka, K. Uchida, S. Kobatake and Y. Shindo, *Chem. Commun.*, 1999, 747